Laser excitation combined with 2*p* photoionization and Auger decay of potassium

K. Jänkälä,[1,*] R. Sankari,[1] J. Schulz,[1,2] M. Huttula,[1] A. Caló,[1] S. Heinäsmäki,[1] S. Fritzsche,[3] T. Rander,[2] S. Svensson,[2] S. Aksela,[1] and H. Aksela[1]

[1]*Department of Physical Sciences, P.O. Box 3000, 90014 University of Oulu, Finland*

[2]*Department of Physics, Uppsala University, Box 530, SE-75121 Uppsala, Sweden*

[3]*Department of Physics, University of Kassel, Heinrich-Plett-Strasse 40, D-34132 Kassel, Germany*

(Received 17 November 2005; published 27 February 2006)

The $2p$ photoionization and subsequent $L_{2,3}M_{2,3}M_{2,3}$ Auger decay spectra from free $4s_{1/2} \rightarrow 4p_{1/2}$ laser-excited potassium atoms are studied both experimentally and theoretically. The shake-up-structure of the $2p$ photoelectron spectrum of K is resolved. A direct experimental way for resolving the satellite structure due to conjugate shake-up transitions accompanying the hole creation in the $L_{2,3}M_{2,3}M_{2,3}$ Auger spectrum of nonexcited atoms is presented. Theoretical *ab initio* computations based on the multiconfiguration Dirac-Fock approach were performed to interpret the experimental findings.

DOI: 10.1103/PhysRevA.73.022720 PACS number(s): 32.80.Hd, 32.80.Rm, 32.80.Bx

I. INTRODUCTION

High resolution x-ray photoelectron spectroscopy and Auger spectroscopy are well established tools to explore the electronic structure of atoms and the quantum mechanical transition processes. For understanding the fine structure of the Auger decay it is valuable to know the distribution of the initial core hole states. While it is complicated to get this information using electron impact ionization the initial state contribution can be measured with x-ray excitation by recording the photoelectron spectrum. In this paper we combined the techniques of synchrotron based x-ray photoelectron spectroscopy with electron impact excited Auger studies in order to get a complete picture of the underlying processes. Even more insight into the Auger decay can be gained by preparing the atoms into different initial states by the means of laser pumping. The valence shell of the atoms can be laser excited before the core ionization. This leads to an occupation of those states that are occupated by the conjugate shake-up process in core excitation from the ground state. We show in this work that the difference spectrum of Auger spectra from laser-excited and ground state atoms can give an experimental Auger spectrum from the valence excited initial states.

First experiments combining laser excitation with photoelectron spectroscopy on free atoms have been performed on atomic sodium in the 1980s [1,2] but only recently the combination with high resolution synchrotron sources allowed us to study the photoemission fine structure in detail [3–5]. These experiments on Na [3] and Rb [5] showed that the photoemission from laser-excited states can help to understand the angular momentum coupling and configuration interaction in the ionic states. To the best of our knowledge, laser excitation has been combined with electron beam excited Auger spectoscopy in 1997 by Dorn and co-workers for Na [6,7] and in 1999 by Zatsarinny *et al.* for Li and Ba [8].

The nonlaser $2p$ photoelectron spectrum of K has been previously studied by Banna *et al.* [9], but the resolution at that time was modest compared to present measurements. The nonlaser $L_{2,3}M_{2,3}M_{2,3}$ Auger electron spectrum of potassium has been measured over 25 years ago by Breuckmann [10] and later by Aksela *et al.* [11]. In these works, Auger electron lines were resolved with good accuracy, but the spectrum shows several high intensity satellite lines which have been previously discussed [9,10], but not assigned reliably.

Measuring the Auger spectra with the laser on and the laser off, and subtracting the laser off spectrum from the spectrum recorded with the laser on, gives a difference spectrum, which can be regarded as an Auger spectrum from laser-excited atoms only. This method requires high resolution and especially high intensity to give reliable results, because the portion of the laser-excited atoms is only between 5–20%.

$L_{2,3}M_{2,3}M_{2,3}$ Auger transitions in nonexcited K can be written as

$$\mathrm{K}(4s^1) + h\nu_S \rightarrow \mathrm{K}^+(2p^5 4s^1) + e^-_{Ph} \rightarrow \mathrm{K}^{2+}(3p^4 4s^1) + e^-_A, \tag{1}$$

where $h\nu_S$ denotes the photon from synchrotron and e^-_{Ph} and e^-_A are the photoelectron and Auger electron, respectively. The Auger spectrum often displays a complicated satellite structure due to shake transitions related either to the photoionization or to the decay process. For the *LMM* Auger spectrum of potassium, a typical shake-up process accompanying the hole creation can be written as

$$\begin{aligned}\mathrm{K}(4s^1) + h\nu_S &\rightarrow \mathrm{K}^{+*}(2p^5 4s^0 nl^1) + e^-_{Ph} \\ &\rightarrow \mathrm{K}^{2+*}(3p^4 4s^0 nl^1) + e^-_A,\end{aligned} \tag{2}$$

where nl denotes the orbital unoccupied in the ground state of K. If $nl = 5s, 6s\ldots$, the photoionization is accompanied by monopole shake transitions and if $nl = 4p, 5p\ldots$, by conjugate transitions. Note that, in principle, the excited electron can change its quantum state also during the Auger decay.

Using a tunable laser one can select a specific excited initial state and increase the intensity of the corresponding Auger electron lines in the spectra. For laser-excited potas-

*Electronic address: kari.jankala@oulu.fi

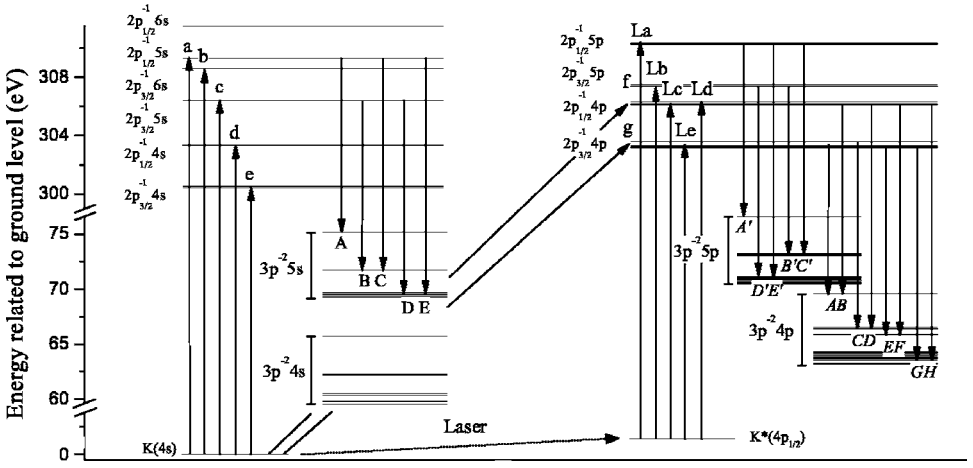

FIG. 1. Energy levels of K($4s$), K*($4p_{1/2}$), K($2p^{-1}[4s,4p,5p,5s,6s]$), and K($3p^{-2}[4s,5s,4p]$) states, computed in the single configuration approximation. All energies are taken relative to the total energy of the ground state (−16 368 eV). Arrows labeled as $a-g$ denote the $2p$ photoinization from the ground state and A–E the subsequent Auger decay of $2p^{-1}5s$ state, whereas labels La–Le stand for the corresponding photoionization transitions of laser-excited K. In the rightmost diagram labels $A-H$ stand for the Auger decay of $2p^{-1}4p$ state and $A'-E'$ denote the Auger decay of $2p^{-1}5p$ state.

sium, the Auger decay process is described by

$$\begin{aligned} \mathrm{K}(4s^1) + h\nu_L &\rightarrow \mathrm{K}^*(4s^0nl^1) + h\nu_S \\ &\rightarrow \mathrm{K}^{+*}(2p^5 4s^0 nl^1) + e^-_{Ph} \\ &\rightarrow \mathrm{K}^{2+*}(3p^4 4s^0 nl^1) + e^-_A, \end{aligned} \tag{3}$$

where $h\nu_L$ is the exciting laser photon and in the present case nl is $4p_{1/2}$. It can be seen from Eqs. (2) and (3) that laser excitation can increase the contribution of the initial states in the Auger spectrum, which correspond to the conjugate shake-up satellites in the ionization process. Therefore, the difference between the nonexcited and the laser-excited Auger spectra can be used to indentify the satellites caused by conjugate shake transitions during the photoionization. In the nonlaser Auger spectrum these lines have low intensity and they merge easily to the backround, but using laser excitation these lines become easier to observe.

Alkali-metal atoms are good model systems to explore the posibilities of the method because of their simple valence shell structure. In this work we report the $2p^{-1}$ photoelectron and subsequent Auger spectra of nonexcited and laser-excited potassium. The experimental spectra are compared to a set of multiconfigurion Dirac-Fock (MCDF) calculations.

II. CALCULATIONS

Calculations of the initial, intermediate, and final states of the transitions given by Eqs. (1)–(3) were carried out in the MCDF model by applying the GRASP92 code [12] in the average level scheme together with the RELCI extension [13]. In the MCDF model, the atomic state functions are formed as linear combinations of jj-coupled configuration state functions (CSF) of the same symmetry, i.e., the same total angular momentum and parity, and are optimized on the basis of the many-electron Dirac-Coulomb Hamiltonian. The CSF are constructed from antisymmetrized products of a common set of orthonormal radial orbitals, represented on some numerical mesh, for which initial estimates were obtained using the Thomas-Fermi model. Further relativistic corrections to the electron-electron interaction are added later in a second step by diagonalizing the Dirac-Coulomb-Breit Hamiltonian matrix. Energy levels obtained from these computations are shown in Fig. 1 for both, the initially laser-exited $4s \rightarrow 4p$ configurations as well as for those without laser excitation.

For nonexcited K, the main electron correlation effects were included by allowing the mixing of the $2p^{-1}3d$ and $2p^{-1}4s$ configurations as well as of the $3p^{-2}3d$ and $3p^{-2}4s$ configurations for the ionic states involved in the photoionization and in the Auger transitions. All other computations were made in the single configuration approximation.

Photoionization cross sections to unexcited and excited states, i.e., K($4s$) and K*($4p_{1/2}$) states were estimated by using an approximative method, where ionization probabilities are obtained by weight factors of the initial state configurations in the final states of photoionization. For more details of this method, see the Appendix of Ref. [14]. Relative intensities for monopole shake-up transitions were estimated by computing overlap integrals between the outer electron's orbitals generated in the initial and final states of the transitions.

To calculate the Auger rates and natural widths related to the transitions, the AUGER component of the RATIP package [15] has been applied. In this component, the continuum spinors are solved within a spherical but level-dependent potential of the final ion (the so-called *optimal level* scheme); this scheme also includes the exchange interaction of the emitted electron with the bound-state density. In practice, the generation of the final scattering states is often a nontrivial task since, apart from the (one-electron) continuum spinors, the appropriate construction of these states also requires the knowledge about the scattering phases and the correct boundary conditions for ionizing processes. Moreover, the number of the possible scattering states of open-shell atoms increases rapidly as the free electron may couple in quite a different ways to its bound-state electrons.

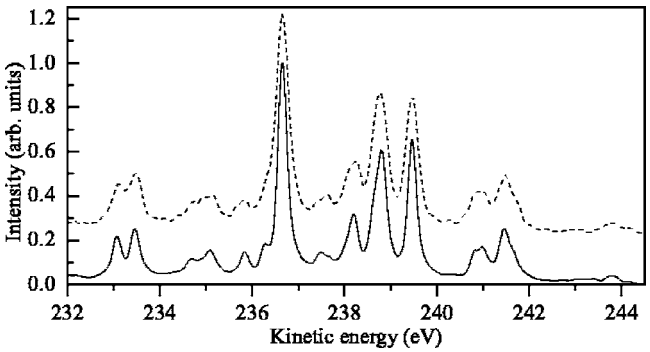

FIG. 2. Experimental *LMM* Auger spectrum of K, measured using synchrotron radiation (dashed line) and electron impact ionization (solid line).

For the computation of relative intensities and level widths, however, neither the relative phases of the continuum spinors are needed nor does the rearrangement of the electron density plays an essential role. In the present computations, therefore, we only included the initial and final-ionic state configuration interactions but omitted the fact that the initial and final-state orbitals are not quite orthogonal to each other following the relaxation of the electron density. In such a "frozen-orbital approach" for the evaluation of the Auger matrix, the transition operator for the autoionization of an excited atomic state, incorporating the full Dirac-Coulomb Hamiltonian, is reduced then to the two-electron Coulomb repulsion as applied in many Auger computations before. For further details on the computations of the Auger matrix elements and relative intensities, we refer the reader to Refs. [16,17].

III. EXPERIMENT

Measurements using synchrotron radiation were carried out at the undulator beamline I411 [18], at the third-generation storage ring MAX II, Lund, Sweden. Synchrotron radiation was monochromatized to the selected photon energy by an SX-700 plane grating monochromator and the emitted electrons were measured with the experimental setup built in Oulu [19], which has been upgraded by replacing the electron spectrometer with a Scienta SES-100 hemispherical electron energy analyzer.

The photo and Auger electron spectra were measured at the magic angle of 54.7° relative to the polarization direction of the synchrotron radiation, with a pass energy of 50 eV. With the settings used, the spectrometer broadening was estimated to be about 250 meV. Auger spectra were also measured with the same electron analyzer, but using a commercial electron gun, made by Specs, for creation of the core hole. The analyzer entrance slit used in the measurements for electron impact ionization was half of the width used in the synchrotron radiation ionization. Otherwise analyzer settings were the same.

The beam of atomic potassium was generated using a resistively heated oven at the temperature of about 210 °C. The $4s_{1/2} \rightarrow 4p_{1/2}$ excitation of atomic potassium was done by using a linearly polarized laser beam with a polarization angle of 90° with respect to the synchrotron beam polarization. The laser system used was a vanadate laser pumped continuous wave Ti:Sa laser.

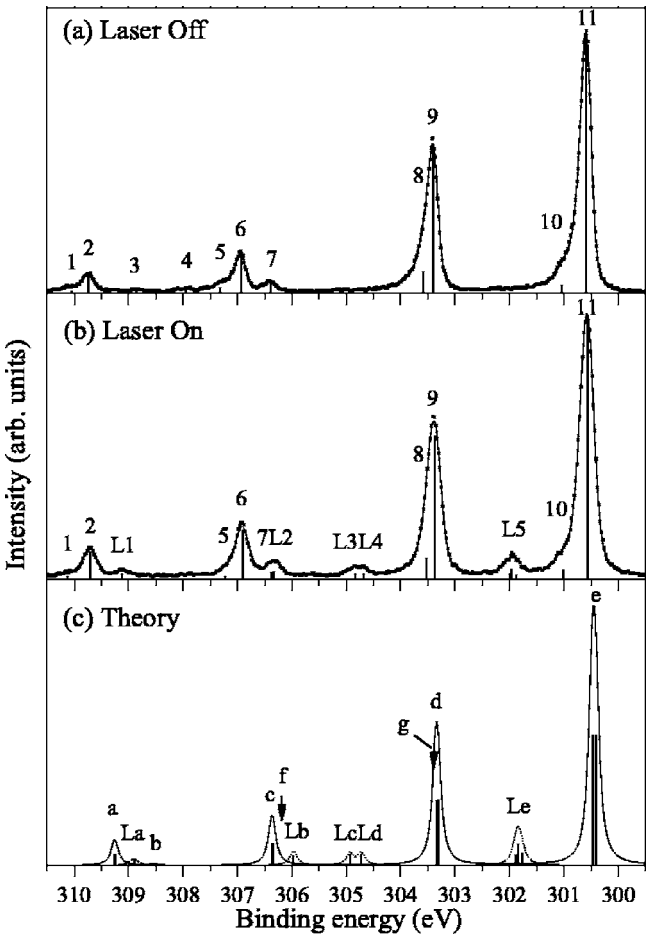

FIG. 3. (a) Experimental $2p^{-1}$ photoelectron spectrum of K; (b) experimental $2p^{-1}$ photoelectron spectrum of K, measured with $4s \rightarrow 4p_{1/2}$ laser excitation; (c) theoretical spectra, the solid line is the $2p^{-1}$ spectrum of K($4s$), the dotted line is the $2p^{-1}$ spectrum of $K^*(4p_{1/2})$, and two arrows denote the energies of computed conjugate $4s \rightarrow 4p$ shake-up lines. For more details, see Fig. 1 and Table I.

The Auger spectra were recorded using synchrotron radiation and electron impact to generate the core ionized states. The spectra obtained with both methods are plotted in Fig. 2. For better visualization the zero level of the spectrum measured using synchrotron radiation is set to 0.23 in the units used. The analysis of the spectral features show small differences in the intensites, but these deviations are not essential for the present study. Since the ionization rate is considerably higher using electron impact ionization a better statistic could be obtained with the electron gun. Thus the Auger spectra for the following analysis have been taken with electron excitation.

The kinetic energy calibration for the Auger spectra seen in Fig. 2 was obtained from Ref. [11], by using the strongest line. For photoelectron spectra the binding energy calibration was obtained from Ref. [9] using peak 11. The presented experimental data consist of sums of several separate spectra.

TABLE I. Experimental and theoretical energies and intensities of K the $2p^{-1}$ photoelectron lines.

Label			Relative intensities			Binding energy (eV)		
Expt.	Theory	Assignment	Expt. 1	Expt. 2	Theory	Expt. 1	Expt. 2	Theory
2	*a*	$4s_{1/2} \rightarrow 2p_{1/2}^{-1}5s_{1/2}$	0.06	0.09	0.08	309.74	309.73	309.26
6	*c*	$4s_{1/2} \rightarrow 2p_{3/2}^{-1}5s_{1/2}$	0.14	0.19	0.17	306.93	306.92	306.38
7	*f*	$4s_{1/2} \rightarrow 2p_{1/2}^{-1}4p_{1/2,3/2}$	0.04	0.02		306.37	306.35	306.20
8	*g*	$4s_{1/2} \rightarrow 2p_{3/2}^{-1}4p_{1/2,3/2}$	0.08	0.10		303.56	303.54	303.30
9	*d*	$4s_{1/2} \rightarrow 2p_{1/2}^{-1}4s_{1/2}$	0.52	0.50	0.50	303.39	303.39	303.35
11	*e*	$4s_{1/2} \rightarrow 2p_{3/2}^{-1}4s_{1/2}$	1	1	1	300.58	300.58	300.46
*L*1	La	$4p_{1/2} \rightarrow 2p_{1/2}^{-1}5p_{1/2,3/2}$		0.22	0.16		309.13	308.93
*L*2	Lb	$4p_{1/2} \rightarrow 2p_{3/2}^{-1}5p_{1/2,3/2}$		0.31	0.31		306.40	306.00
*L*3/*L*4	Lc/Ld	$4p_{1/2} \rightarrow 2p_{1/2}^{-1}4p_{1/2,3/2}$		0.50	0.50		304.77	304.86
*L*5	Le	$4p_{1/2} \rightarrow 2p_{3/2}^{-1}4p_{1/2,3/2}$		1	1		301.96	301.86

All the individual spectra were recorded in pairs of lasers on and off, in order to keep the experimental parameters the same between the laser-excited and nonexcited spectra.

IV. RESULTS AND DISCUSSION

A. $2p^{-1}$ photoelectron spectra of laser-excited and nonexcited atomic K

Experimental $2p^{-1}$ photoelectron spectra of K taken with lasers on and off are plotted in Figs. 3(a) and 3(b). The laser-off spectrum was measured using photon energies of 340 and 400 eV. No essential differences were obtained, but the resolution is slightly better in the 340 eV spectrum and therefore it will be used in the following. The spectrum in Fig. 3(a) has been fitted with 11 asymmetric Voigt functions [20] in order to take post collision interaction (PCI) effect into account.

Peaks 2, 6, 9, and 11 have been previously assigned in Ref. [9], but due to a modest resolution, the other lines were not seen. The main $2p_{1/2,3/2}^{-1}$ photoemission peaks in the experimental spectra in Fig. 3 are labeled as 9 and 11. At higher binding energy, peaks 2 and 6 are due to $4s \rightarrow 2p_{1/2,3/2}^{-1}5s$ monopole shake-up transitions. Using the energy levels presented in Fig. 1 and the spectra in Fig. 3(c) we are able to identify peaks 7 and 8 as the $4s \rightarrow 2p_{1/2,3/2}^{-1}4p$ conjugated shake-up transitions. Peak 3 can be identified as the $4s \rightarrow 2p_{3/2}^{-1}6s$ monopole shake-up transition, the $4s \rightarrow 2p_{1/2}^{-1}6s$ line lies out of the measured energy range. The peaks 1, 4, 5, and 10 remained unidentified.

The energy separation of the shake-up lines is the same as the corresponding separation of the main lines. Therefore, the distance between peaks 2 and 6, and also between lines 7 and 8 were fixed to be equal to the energy difference between the lines 9 and 11 [see Fig. 3(a)]. Experimental energies and intensities are given in Table I together with the calculated values.

In a single configuration scheme, the $2p$ photoionization of K($4s$) leads to four core-hole states. These states can be written using jj coupling as $2p_{1/2}^{-1}4s_{1/2}[1/2]_{0,1}$ and $2p_{3/2}^{-1}4s_{1/2}[3/2]_{1,2}$. Lines divide into two doublets denoted by d and e in Figs. 1 and 3(c) corresponding to a $2p$ hole with total angular momenta of $j=\frac{1}{2}$ and $j=\frac{3}{2}$. The fine structure of the lines is not resolved in the experimental spectrum due to a very small splitting (50 meV) of the states compared to their lifetime widths (150 meV). The inclusion of the $2p^{-1}3d$ configuration incerases the number of computed lines to 16, but due to a very small mixing of configurations no significant changes in the spectrum were seen.

The spectrum measured with laser on in Fig. 3(b) was done by using a photon energy of 400 eV. Differences caused by laser excitation are seen as new peaks in the spectrum, labeled as $L1-L5$. The fitting procedure was the same as before, with a small exception that the difference between peaks $L1$ and $L2$ was fixed to be the same as the difference between peak $L5$ and the average of peaks $L3$ and $L4$.

The main peaks due to the laser excitation labeled as $L3$, $L4$, and $L5$ in Fig. 3(b), correspond to Lc/Ld and Le in Fig. 3(c). The structure $L3/L4$ corresponds to the $2p_{1/2}^{-1}4p$ hole and $L5$ corresponds to $2p_{3/2}^{-1}4p$ hole. Replacing the $4s_{1/2}$ valence electron by the $4p$ leads to a large energy splitting of the jj-coupled $2p_{1/2}^{-1}4p_{1/2}[1/2]_{0,1}$ states, giving rise to peaks Lc and Ld in Fig. 3(c), as compared to the splitting of the states $2p_{1/2}^{-1}4s_{1/2}[1/2]_{0,1}$ forming the nonexcited doublet d. The estimated increase in spitting is confirmed by experiment, where peaks $L3$ and $L4$ are resolved.

Due to a mixing of the jj-coupled states $2p_{3/2}^{-1}4p_{1/2}[3/2]_1$ and $2p_{3/2}^{-1}4p_{3/2}[3/2]_1$, the latter state is also populated in the photoionization of $K^*(4p_{1/2})$. The $2p_{3/2}^{-1}4p_{1/2}[3/2]_2$ state stays independent. Therefore, peak Le is created by transitions to three different final states. Two of the states correspond to the total angular momenta of $J=1$ and one state to $J=2$. In the experimental spectrum [Fig. 3(b)], three lines were indeed needed to account for the fine structure of $L5$ when fitting the data. The computed splitting 110 meV of two $J=1$ states agrees well with the 130 meV obtained from the fit. By comparison of peaks $L1$ and $L2$ to the computed peaks La and Lb, $L1$ and $L2$ can be identified as $4p_{1/2} \rightarrow 2p_{1/2,3/2}^{-1}5p$ monopole shake-up transitions from the excited K.

The computed energies of the transitions shown in Fig. 1 and the theoretical spectrum in Fig. 3(c), predict the lines

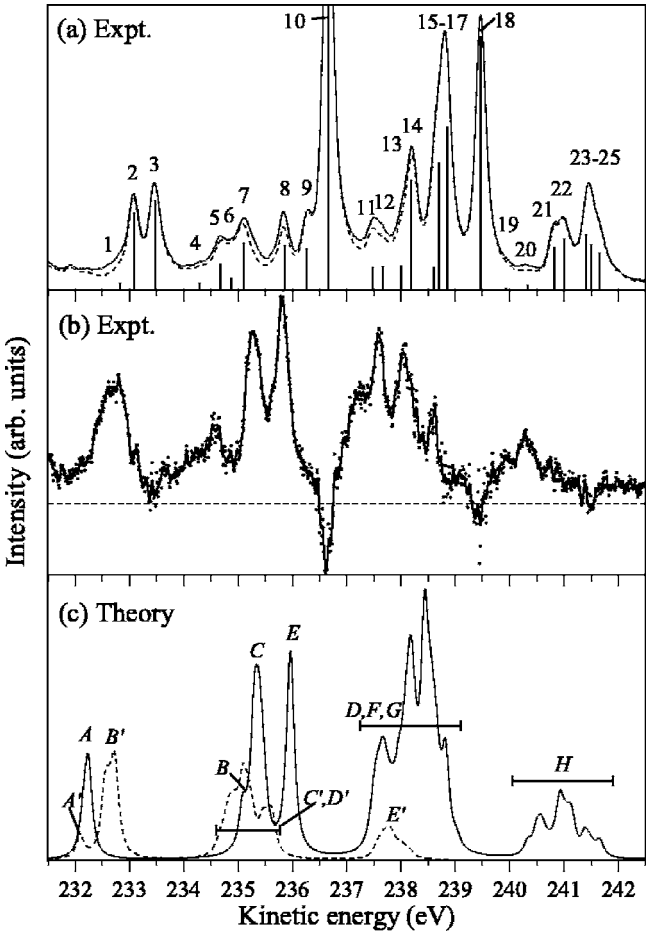

FIG. 4. (a) Experimental potassium *LMM* Auger spectra measured with laser on (solid line) and off (dashed line); (b) a difference spectrum taken between the laser on and off spectra shown in upper panel. The dashed line denotes the zero level. (c) The solid line represents the theoretical $2p^{-1}4p \rightarrow 3p^{-2}4p$ Auger spectrum and the dashed line the theoretical $2p^{-1}5p \rightarrow 3p^{-2}5p$ Auger spectrum.

seen in the experimental spectra in the upper panels quite well. The intensity of the laser-excited states depends mostly on the laser alignment and the properties of the selected atom. Therefore, the relative intensities for unexcited and excited atoms in Table I are given with respect to peaks 11 and *L*5 separately. For visualization the spectrum corresponding excited K [Fig. 3(c)] is scaled down. The energies of peaks corresponding to the $4s \rightarrow 2p^{-1}_{1/2,3/2}4s$ and $4p_{1/2} \rightarrow 2p^{-1}_{1/2,3/2}4p$ transitions are predicted well by the single configuration approximation (or by including the $4s$-$3d$ mixing only), but the error increases noticeably for the shake-up lines. The prediction of the relative intensites is good, even for monopole shake-up transitions in the laser-excited spectrum.

B. Laser-excited $L_{2,3}M_{2,3}M_{2,3}$ Auger spectrum of K

Figure 4(a) shows the experimental *LMM* Auger spectrum with laser on and off. The nonlaser spectrum is identical to the lower spectrum in Fig. 2. To increase the visibility of the difference, the spectrum is scaled up. The cut line 10 shows no laser contribution.

The total atomic density in the interaction region is practically constant. The laser excitation redistributes the density of atoms by pumping a part of the atoms into the excited states. The efficiency of the laser excitation was found to be about 7%, thus leaving about 93% of the potassium atoms to K($4s$) state. To facilitate the comparison between the laser-excited and nonexcited spectra, the intensity contribution from nonexcited atoms in the laser on spectrum in Fig. 4(a) was normalized, to correspond the spectrum recorded with laser off. The chosen normalization factor (1.07) was the average of the intensity ratios of the peaks 3, 10, and 15–18 in the Auger spectrum of laser-excited and nonexcited K, respectively. Normalization to these peaks can be justified from the computed spectrum presented in Fig. 4(c), which predicts no overlapping peaks in excited and nonexcited spectra in these regions and from the observation that all these peaks have almost the same intensity ratio between laser on and off spectra.

The lines 3, 9, 10, 13–18, and 21–25 were identified to originate from the $2p^{-1}4s \rightarrow 3p^{-2}4s$ transitions already in Ref. [11]. The vertical bars in Fig. 4(a) denote the lines obtained from a fitting procedure of the spectrum measured without laser. Clear changes can be seen in the spectrum obtained with laser on. The peaks that have risen in the laser on the spectrum are 1, 4–8, 11–14, and 19–20. Apart from lines 13 and 14, all observed changes take place in the region of the satellite structures.

The spectrum in Fig. 4(b) displays a difference between the two spectra shown in panel 4(a) and hence presents the experimental Auger spectrum from the laser-excited K. The solid line is the smoothed spectrum obtained by using the Fourier transform in order to reduce the high frequency statistical noise. The dots are original data points and one can estimate the relative error from the scattering of these points. The spectrum has two negative intensity regions at energies 236.5 and 239.5 eV. These structures have no physical meaning, because they are caused by slight differences between laser on and off spectra in the slopes of peaks 10 and of 18.

Theoretical $2p^{-1}4p \rightarrow 3p^{-2}4p$ and $2p^{-1}5p \rightarrow 3p^{-2}5p$ Auger spectra are plotted in Fig. 4(c). The labels of the peaks refer to Fig. 1. Both spectra have been generated using calculated transition energies and intensities. In addition both spectra have been shifted by −1.56 eV in order to coincide with the experimental energies. The shift was taken to be the same as the shift between experimental and theoretical spectra of nonexcited K. The intensity ratio of about 0.35 between the two spectra was obtained from the experimental values given in Table I for the $2p$ photoionization of $K^*(4p_{1/2})$. The ratio $2p^{-1}_{1/2}/2p^{-1}_{3/2}$ for $5p$ excited spectrum was also taken from Table I.

The shifts of the computed spectra are due to incomplete considerations of correlation energies of the initial and final states of the corresponding transitions. An error in correlation energy computations arises from the use of a finite set of basis functions and it changes slightly between different states. The chosen energy shift represents the average of the correlation energy corrections of all the transitions in the corresponding spectra. Therefore, using a constant shift one cannot reproduce all the peaks into exactly experimentally observed energies.

The spectra of the excited and nonexcited K, seen in Fig. 4, display remarkable differences. The computed peaks *C* and *E* in Fig. 4(c), which are also seen clearly in Fig. 4(b) are clearly separated in excited K. These structures correspond to the doublet peak 10 in the nonexcited K. The structures labeled as *D*, *F*, *G*, which correspond to the lines 13–18, and the structure *H* having its counterpart in lines 21–25 differ somewhat in details, thus the excited valence electron causes larger energy splitting, but the main features remain nearly the same.

The $2p^{-1}4p \rightarrow 3p^{-2}4p$ transitions do not explain the experimentally observed structure in the kinetic energy region of 233–235 eV nor the wide peak in the energy region of 232–233 eV. These features arise from the $2p^{-1}5p \rightarrow 3p^{-2}5p$ transitions marked as $A'-D'$, created after the $4p \rightarrow 5p$ monopole shake-up during the ionization. These initial states are also seen in the experimental photoionization spectrum as peaks *L*1 and *L*2 and the observed intensities agree well with the intensity seen in the Auger spectrum. The $2p^{-1}5p \rightarrow 3p^{-2}5p$ spectrum should be shifted a bit more to lower kinetic energy to a better agreement with the experiment. The overlapping satellite spectrum explains also the intensity discrepancies in the energy region of 237–238 eV.

A good agreement between experimental and theoretical spectra is seen when comparing Figs. 4(b) and 4(c), despite the relatively low intensity of the difference spectrum. The energy splittings are fairly well predicted and no considerable discrepancies in intensity distributions between theory and experiment are found.

C. Satellite structure of the $L_{2,3}M_{2,3}M_{2,3}$ Auger spectrum of K

The information obtained from the Auger spectrum of laser-excited K can now be used to assign the structures of the experimental *LMM* Auger spectrum of potassium. From the photoelectron spectrum one can obtain the relative populations of the initial states $2p^{-1}[4s,4p,5s]$ of the Auger transition, all of which fall into the same energy region. In the first approximation, the probability of monopole shake-up transitions does not depend on the ionization energy, but the conjugate shake-up transitions are expected to be stronger at ionization energies close to the threshold (see, e.g., Ref. [21]). It should be noted that the shake probability may also depend on the ionization method, but in this study at least the decay spectrum following photoionization or electron impact ionizations did not show remarkable changes. This observation suggests that the population of the initial states was the same.

In this study, the relative populations of the Auger transition initial states were estimated from the photoelectron spectrum presented in Fig. 3(a). The relative strength of the $2p^{-1}4s$ states was about 0.79 whereas strengths of the $2p^{-1}5s$ and $2p^{-1}4p$ states are about 0.10 and 0.06, respectively. These values were used when constructing the theoretical *LMM* Auger spectrum including some of the satellite structures. The spectrum thus obtained is plotted in the middle panel of Fig. 5. The theoretical Auger spectra originating from $2p^{-1}4s$ and $2p^{-1}4p$ states have been shifted in kinetic energy by −1.56 eV to coincide theoretical and experimental

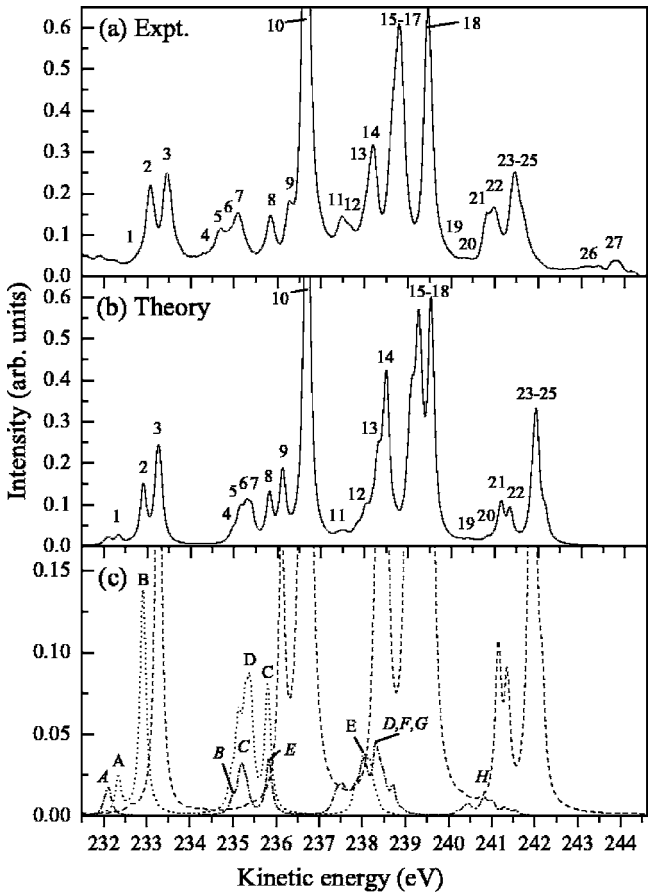

FIG. 5. (a) Experimental *LMM* Auger electron spectrum of K; (b) theoretical spectrum including $2p^{-1}(4s,4p,5s) \rightarrow 3p^{-2}(4s,4p,5s)$ transitions; (c) theoretical $2p^{-1}4s \rightarrow 3p^{-2}4s$ spectrum (dashed line), $2p^{-1}5s \rightarrow 3p^{-2}5s$ (dotted line) and $2p^{-1}4p \rightarrow 3p^{-2}4p$ spectrum (dash dotted line).

spectrum at 236.67 eV [peak 10 in Fig. 5(a)]. The theoretical $2p^{-1}5s \rightarrow 3p^{-2}5s$ Auger spectrum is shifted by −1.82 eV to have the energy difference between the peaks 1 and 2 the same as in the experimental spectrum.

In shake processes accompanying the photoionization, the outermost $4s$ electron can shake either to the $4p_{1/2}$ or $4p_{3/2}$ orbital. Although there is a small difference in the decay spectrum depending whether the excited electron is on the $4p_{1/2}$ or $4p_{3/2}$ orbital, the main features remain the same and conclusions can be drawn on the basis of the Auger spectrum of $K^*(4p_{1/2})$. By comparing the Auger spectra presented in Fig. 4(a), it is obvious that that the lines 1, 4–8, 11–14, 19, and 20 have some contribution from the $K^*(4p_{1/2})$ as all these lines increased when the laser excitation was used. Combining this fact with the existence of the $2p^{-1}4p_{1/2,3/2}$ states in the $2p$ photoelectron spectrum of K($4s$) allows us to conclude that lines 1, 7, 8, 11–14, 19, and 20 originate, at least partly, from $2p^{-1}4p \rightarrow 3p^{-2}4p$ transitions.

However, the intensity of these satellite lines cannot be explained alone by the conjugate shake-up transitions during the $2p$ photoionization. It was seen from the photoelectron spectrum that the most populated satellite state is the $2p^{-1}5s$ state which suggests that most of the satellite structures must also originate from this state. Indeed the theoretical

TABLE II. Identification of the satellite lines.

Label	I	II	III	IV	Label	I	II	III	IV
1			×	×	11		×	×	×
2			×		12		×	×	×
4		×			19				×
5	×	×	×		20				×
6			×		26		×		
7			×		27		×		×
8			×	×					

I: $2p^{-1}4s \rightarrow 3p^{-2}5s$
II: $2p^{-1}4s \rightarrow 3p^{-2}3d$
III: $2p^{-1}5s \rightarrow 3p^{-2}5s$
IV: $2p^{-1}4p \rightarrow 3p^{-2}4p$

$2p^{-1}5s \rightarrow 3p^{-2}5s$ spectrum presented in Fig. 5(c) (dotted line), (see also Fig. 1), shows that, for example, the strong peak 2 in Fig. 5(a) corresponds to theoretical peak *B* and these transitions cause some intensity in the region of peaks 4–8 [features *C* and *D* in Fig. 5(c)] and peaks of 11 and 12 [peak *E* in Fig. 5(c)]. In addition, for example, peaks 4–6, which rise also in the laser-on spectrum, originate also partly from $2p^{-1}5p \rightarrow 3p^{-2}5p$ transitions.

To gain a full understanding of an experimental Auger spectrum, the effect of the mixing of configurations, must also be considered. The final state splittings for the $3p^{-2}3d$ and $3p^{-2}5s$ configurations can be obtained from Ref. [22]. From these values it can be estimated that peaks 26 and 27 are mainly due to the $2p_{1/2}^{-1}4s \rightarrow 3p^{-2}3d$ transitions and lines 11 and 12 get some intensity from this process. The $2p_{3/2}^{-1}4s \rightarrow 3p^{-2}3d$ transition gives rise to peaks 5, 6, and 19.

From optical values it can also be seen that the $2p_{1/2}^{-1}4s \rightarrow 3p^{-2}5s$ transition creates some intensity to lines 5 and 6 and $2p_{3/2}^{-1}4s \rightarrow 3p^{-2}5s$ transition gives rise to a weak peak 1. Shake-up may also take place during the Auger transition, but lines created via shake-up during ionization dominate the spectrum. For example, the theoretical $4s \rightarrow 5s$ monopole shake-up probability in photoionization is about 0.168, but in Auger decay it is only 0.037. All indentifications are summarized in Table II, which shows also the complexity of identifying the satellite structure of an Auger spectrum.

V. CONCLUSIONS

Combining laser excitation to inner-shell photoelectron and Auger spectroscopy is a promising method to investigate details of atomic structure. The effects caused by the laser excitation in the photoelectron spectrum were found to be very well predicted by MCDF calculations. The pure laser-excited Auger spectrum is also in good agreement with the computed spectrum and the predicted increment in splitting of energy levels was detected. Laser excitation was proven to be a useful method for examining complicated satellite structures of an experimental Auger spectrum. The laser excitation together with a theoretical investigation allowed us to assign the satellite structure of the experimental *LMM* Auger spectrum of potassium.

ACKNOWLEDGMENTS

This work has been financially supported by the Reseach Council for Natural Sciences of the Academy of Finland, the Swedish Research Council (VR), the Swedish Foundation for Strategic Research (SSF), and NordForsk. We thank the staff of MAX-lab for help during the measurements.

[1] J. L. Le Gouët, J. L. Picqué, F. Wuilleumier, J. M. Bizau, P. Dhez, P. Koch, and D. L. Ederer, Phys. Rev. Lett. **48**, 600 (1982).
[2] D. Cubaynes, J. M. Bizau, F. J. Wuilleumier, B. Carré, and F. Gounand, Phys. Rev. Lett. **63**, 2460 (1989).
[3] D. Cubaynes, M. Meyer, A. N. Grum-Grizhmailo, J.-M. Bizau, E. T. Kennedy, J. Bozek, M. Martins, S. Canton, B. Rude, N. Berrah, and F. J. Wuilleumier, Phys. Rev. Lett. **92**, 233002 (2004).
[4] J. Schulz, M. Tchaplyguine, T. Rander, O. Björneholm, S. Svensson, R. Sankari, S. Heinäsmäki, H. Aksela, S. Aksela, and E. Kukk, Phys. Rev. A **72**, 010702(R) (2005).
[5] J. Schulz, M. Tchaplyguine, T. Rander, H. Bergersen, A. Lindblad, G. Öhrwall, S. Svensson, S. Heinäsmäki, R. Sankari, S. Osmekhin, S. Aksela, and H. Aksela, Phys. Rev. A **72**, 032718 (2005).
[6] A. Dorn, O. I. Zatsarinny, and W. Mehlhorn, J. Phys. B **30**, 2975 (1997).
[7] J. Nienhaus, O. I. Zatsarinny, A. Dorn, and W. Mehlhorn, J. Phys. B **30**, 3611 (1997).
[8] O. I. Zatsarinny, A. Dorn, H. Lörch, J. Nienhaus, and W. Mehlhorn, Nucl. Instrum. Methods Phys. Res. B **154**, 90 (1999).
[9] M. S. Banna and A. R. Slaughter, Phys. Rev. A **30**, 3021 (1984).
[10] B. Breuckmann, Ph.D. thesis, Freiburg University, 1978 (unpublished).
[11] S. Aksela, M. Kellokumpu, H. Aksela, and J. Väyrynen, Phys. Rev. A **23**, 2374 (1981).
[12] F. A. Parpia, C. Froese Fischer, and I. P. Grant, Comput. Phys. Commun. **94**, 249 (1996).
[13] S. Fritzsche, C. Froese Fischer, and G. Gaigalas, Comput. Phys. Commun. **148**, 103 (2002).
[14] M. Huttula, E. Kukk, S. Heinäsmäki, M. Jurvansuu, S. Fritzsche, H. Aksela, and S. Aksela, Phys. Rev. A **69**, 012702 (2004).
[15] S. Fritzsche, J. Electron Spectrosc. Relat. Phenom. **114**, 1155 (2001).
[16] S. Fritzsche, B. Fricke, and W.-D. Sepp, Phys. Rev. A **45**, 1465 (1992).
[17] S. Fritzsche, Phys. Scr., T **100**, 37 (2002).

[18] M. Bässler, A. Ausmess, M. Jurvansuu, R. Feifel, J.-O. Forsell, P. de Tarso Fronseca, A. Kivimäki, S. Sundin, and S. L. Sorensen, Nucl. Instrum. Methods Phys. Res. A **469**, 382 (2001).
[19] M. Huttula, M. Harkoma, E. Nõmmiste, and S. Aksela, Nucl. Instrum. Methods Phys. Res. A **467–468**, 1514 (2001).
[20] P. van der Straten, R. Morgenstern, and A. Niehaus, Z. Phys. D: At., Mol. Clusters **8**, 35 (1988).
[21] W. T. Cheng, E. Kukk, D. Cubaynes, J.-C. Chang, G. Snell, J. D. Bozek, F. J. Wuilleumier, and H. Berrah, Phys. Rev. A **62**, 062509 (2000).
[22] C. E. Moore, *Atomic Energy Levels*, Natl. Bur. Stand. Circ. No. 467 (U.S. GPO. Washington D.C., 1949), Vol. 1.